Structure and Luminescence of Eu^{3+}-Doped Class I Siloxane−Poly(ethylene glycol) Hybrids

C. Molina,† K. Dahmouche,† C. V. Santilli,† A. F. Craievich,‡ and S. J. L. Ribeiro*,†

Institute of Chemistry, UNESP, P.O.Box 355, 14801-970, Araraquara SP, Brazil, and Institute of Physics, USP, São Paulo, Brazil

Received November 27, 2000. Revised Manuscript Received April 24, 2001

Transparent, flexible, and luminescent Eu^{3+}-doped siloxane−poly(ethylene glycol) (PEG) nanocomposites have been obtained by the sol−gel process. The inorganic (siloxane) and organic PEG phases are usually linked by weak bonds (hydrogen bonds or van der Waals forces), and small-angle X-ray scattering (SAXS) measurements suggest that the structure of these materials consists of fractal siloxane aggregates embedded in the PEG matrix. For low Eu^{3+} contents, $n = 300$ and $n = 80$, the aggregates are small and isolated and their fractal dimensions are 2.1 and 1.7, respectively. These values are close to those expected for gelation mechanisms consisting of reaction-limited cluster−cluster aggregation (RLCCA) and diffusion-limited cluster−cluster aggregation (DLCCA). For high Eu^{3+} content, SAXS results are consistent with a two-level structure: a primary level of siloxane aggregates and a second level, much larger, formed by the coalescence of the primary ones. The observed increase in the glass transition temperature for increasing Eu^{3+} content is consistent with the structural model derived from SAXS measurements. Extended X-ray absorption fine structure (EXAFS) and luminescence spectroscopy measurements indicate that under the experimental conditions utilized here Eu^{3+} ions do not strongly interact with the polymeric phase.

1. Introduction

Inorganic−organic hybrid materials have emerged in the last years as potential interesting hosts in different technological fields such as optics, electronics, mechanics, and biology.[1,2] In general, the main interest of these molecular-scale composite materials basically derives from the possibility of tailoring the properties of novel multifunctional advanced materials through the combination at the nanosize level of the organic and inorganic components in a single material.[3−5] Following Sanchez and Ribot, these materials can be divided in two main classes:[3] (a) In the so-called "class I hybrids" the organic and inorganic phases are linked together through weak interactions (hydrogen, van der Waals, or ionic bonds), which give cohesion to the whole structure; that is, they are physical hybrids. (b) The "class II hybrids" are also biphasic materials with the difference that strong covalent bonds link the organic and inorganic parts. They are chemical hybrids.

In particular, siloxane−polyether hybrids offer high visible transparency, flexibility, and good chemical stability. When these materials are prepared containing Eu^{3+}, potentially interesting phosphors are obtained. Eu^{3+}-doped class II hybrids exhibit a multiwavelength emission, where a broad band intrinsic to the hybrid host is superposed to a series of yellow-red narrow Eu^{3+} lines.[6−10] The Eu^{3+} local order and the influence of europium doping on the structure of these composites has also been studied.[6−10] Interestingly enough, the nature of the Eu^{3+} first coordination shell in these hybrids may be tuned, as a function both of the salt concentration and of the polymer molecular weight.[10] In hybrids containing relatively long organic segments, Eu^{3+} ions interact mainly with the carbonyl-type oxygen atoms of the urea cross-links located at the organic/inorganic interface. On the other hand, in hybrids containing shorter polymer chains the lanthanide ions are unable to disrupt the characteristic strong and

* To whom correspondence should be addressed. Tel.: 55-16-2016631. Fax: 55-16-2227932. E-mail- sidney@iq.unesp.br.
† Institute of Chemistry.
‡ Institute of Physics.

(1) Schmidt, H. K. *J. Sol−Gel Sci. Technol.* **1997**, *8*, 557.
(2) Seddon, A. B. Potential of Organic−Inorganic Hybrid Materials, derived by Sol−Gel, for Photonic Applications. In *Sol−Gel and Polymer Photonic Devices*; Critical Review of Optical Science and Technology Series; SPIE Optical Engineering Press: Bellingham, WA, 1997; Vol. CR68, pp 143−171.
(3) Sanchez, C.; Ribot, F. *New J. Chem.* **1994**, *18*, 1007.
(4) Judeinstein, P.; Titman, J.; Stamm, M.; Schmidt, H. *Chem. Mater.* **1994**, *6*, 127.
(5) Carlos, L. D.; de Zea Bermudez, V.; Duarte, M. C.; Silva, M. M.; Silva, C. J.; Smith, M. J.; Assunção, M.; Alcácer, L. In *Physics and Chemistry of Luminescent Materials VI*; Ronda, C., Welker, T., Eds.; Electrochemical Society Proceedings, San Francisco, 1998; Vol. 97-29, p 352.
(6) Ribeiro, S. J. L.; Dahmouche, K.; Ribeiro, C. A.; Santilli, C. V.; Pulcinelli, S. H. *J. Sol-Gel Sci. Technol.* **1998**, *13*, 427.
(7) Carlos, L. D.; de Zéa Bermudez, V.; Sá Ferreira, R. A.; Marques, L.; Assunção, M. *Chem. Mater.* **1999**, *11*, 581.
(8) Molina, C.; Ribeiro, S. J. L.; Dahmouche, K.; Santilli, C. V.; Craievich, A. F. *J. Sol-Gel Sci. Technol.* **2000**, *19*(1−3), 615.
(9) (a) Carlos, L. D.; Sá Ferreira, R. A.; de Zea Bermudez, V.; Molina, C.; Bueno, L. A.; Ribeiro, S. J. L *Phys. Rev. B* **1999**, *60*, 10042. (b) Carlos, L. D.; Messaddeq, Y.; Brito, H. F.; Sá Ferreira, R. A.; de Zea Bermudez, V.; Ribeiro, S. J. L. *Adv. Mater.* **2000**, *12*, 594.
(10) (a) de Zea Bermudez, V.; Sá Ferreira, R. A.; Carlos, L. D.; Molina, C.; Dahmouche, K.; Ribeiro, S. J. L. *J. Phys. Chem. A*, in press.

10.1021/cm0012320 CCC: $20.00
Published on Web 08/30/2001

ordered hydrogen-bonded urea−urea structures and, therefore, the preferential coordination sites are the ether−oxygen atoms of the polymer chains.[6−10]

Small-angle X-ray scattering (SAXS) has been utilized to study the structural features of nondoped class I and class II siloxane−poly(ethylene glycol) (PEG) composites.[11,12] The experimental results indicated that class I hybrids are composed of fractal siloxane clusters embedded in the polymer matrix, while in class II composites small isolated and spatially correlated siloxane particles are formed within the polymeric matrix.

In this paper we present results on the structural characteristics of class I Eu^{3+}-doped siloxane−PEG nanocomposites. Thermal analysis, small-angle X-ray scattering (SAXS), extended X-ray absorption fine structure (EXAFS) at the Eu^{3+} L_{III} edge, and Eu^{3+} luminescence results are presented and compared with previous results presented in the literature.[13,14] Strong dependence of the Eu^{3+} luminescence properties on the nature of the polymeric counterpart and on preparation experimental conditions are suggested.

2. Experimental Section

2.1. Samples and Techniques. Class I hybrids were prepared by an ultrasonic-assisted sol−gel method to promote the miscibility of reactants. Tetraethoxysilane (TEOS) and hydrochloric acid aqueous solution (0.1 mol L^{-1}) were stirred together under ultrasound for 5 min ($[H_2O]/[TEOS] = 4$). Poly(ethylene glycol), PEG_{600} (600 being the molecular weight of PEG), was added to the silica sol under ultrasound. To compare the results with previous ones obtained for class II hybrids,[8] the polymer relative concentration was kept at 86% in weight. An ethanolic solution of Eu^{3+} perchlorate was added to the hybrid to obtain several doping contents. The Eu^{3+} content is expressed here, as usual in polymer science, as the ratio between the number of ether-type oxygen atoms and Eu^{3+} atoms ($n = [O]/[Eu] = 8, 15, 30, 80, 300$). Gels were obtained by pH increasing with the addition of NH_4OH solution (pH = 8). Xerogels were obtained by heat treatment at 50 °C for 24 h.

The glass transition temperatures (T_g) of the hybrids were determined as a function of Eu^{3+} content using thermomechanical analysis (TMA) performed with a 2940 TA Instruments apparatus from −100 to 100 °C (heating rate of 10 °C/min) under a N_2 atmosphere and a 0.05 N charge.

The small-angle X-ray scattering study was performed using the SAS synchrotron beamline of the Brazilian National Synchrotron Laboratory-LNLS (www.lnls.br). The beamline is equipped with an asymmetrically cut and bent silicon (111) monochromator that yields a monochromatic ($\lambda = 1.68$ Å) and horizontally focused beam. A vertical position-sensitive X-ray detector and a multichannel analyzer were used to record the scattering intensity, $I(q)$, as a function of the modulus of the scattering vector $q = 4\pi \sin(\epsilon/\lambda)$, with ϵ being the scattering angle. Each SAXS spectrum corresponds to a data collection time interval of 300 s.

Luminescence data (excitation and emission spectra and excited-state decay times) were obtained under both continuous (450 W) and pulsed (5 J/pulse, 3-μs bandwidth) Xe lamps excitation with a SPEX Fluorolog F2121 spectrofluorimeter. All measurements were obtained in the front face acquisition mode at room temperature. Decay curves were processed with the SPEX 1934 phosphorimeter.

The X-ray absorption experiments (EXAFS) were conducted using the XAFS beamline of LNLS. A Si(111) two-crystal monochromator was used. Spectra were recorded close to the Eu L_{III} edge (6983 eV) in the fluorescence mode. An air-filled ionization chamber was used to monitor the X-ray beam intensity on the sample and a NaI detector was used to detect the fluorescence signal. An Eu^{3+} aqueous solution (pH = 4) was used as a reference for the simulations of the first coordination sphere around the Eu^{3+} atom (8.6 oxygen atoms and the distance of 2.43 Å).[15]

2.2. Scattering Function of Fractal Aggregates (Theory). The scattering function $I(q)$ of an isotropic system composed of spatially correlated primary particles is given by[16]

$$I(q) = \phi P(q) S(q) \tag{1}$$

where ϕ is the number of primary particles per unit volume, $P(q)$ is the form factor of the primary particles, and $S(q)$ is the effective structure function that accounts for the spatial correlation between them.

The structure function for a set of correlated primary particles forming a fractal object[17] is given by[18,19]

$$S(q) = \left(1 + \left\{\left[\frac{1}{(qa)^D}\right] \times \left\{\frac{[D\cdot\Gamma(D-1)]}{\left[1 + \left(\frac{1}{q^2\xi^2}\right)\right]^{(D-1)/2}}\right\} \times \sin[(D-1)\tan^{-1}(q\xi)]\right\}\right) \tag{2}$$

where a is the radius of the (assumed spherical) primary particles, ξ is the correlation length of the fractal structure, D is the fractal dimension, and Γ is the gamma function.

For very small primary particles ($a \ll \xi$), the form factor $P(q)$ can be approximated by Guinier law,[16]

$$P(q) = (\rho_p - \rho_m)^2 v^2 e^{(-a^2q^2)/5} \tag{3}$$

where ρ_p is the electronic density of the (assumed homogeneous) primary particles, v their volume, and ρ_m the electronic density of the medium where the particles are embedded.

Assuming that (i) the composite material is composed of isolated fractal aggregates, without spatial correlation between them, and (ii) the aggregates consist of very small primary particles ($a \ll \xi$) with volume v and electronic density contrast $\Delta\rho = (\rho_p - \rho_m)$, the scattering function can be written as

$$I(q) = \phi(\Delta\rho)^2 v^2 e^{(-a^2q^2)/5} S(q), \text{ that is,}$$

$$I(q) = A e^{(-a^2q^2)/5} S(q) \tag{4}$$

where $S(q)$ is given by eq 2 and A is a constant. Equation 4 becomes $I(q) \propto q^{-D}$ for $1/\xi \ll q \ll 1/a$ and exhibits "crossover" points at $q_1 = 1/\xi$ and $q_2 = 1/a$.

At small q ($q \leq 1/\xi$), $I(q)$ exhibits Guinier-type behavior.[16] The radius of gyration of the isolated fractal aggregates, R_g, is related to the correlation length ξ by

$$R_g = \left[\frac{D(D+1)}{2}\right]^{1/2} \xi \tag{5}$$

(11) Dahmouche, K.; Santilli, C. V.; Pulcinelli, S. H.; Craievich, A. F. *J. Phys. Chem. B* **1999**, *103*, 4937.
(12) Chaker, J.; Dahmouche, K.; Santilli, C. V.; Pulcinelli, S. H.; Craievich, A. F. *J. Appl. Crystallogr.* **2000**, *33*(1), 700.
(13) (a) Bekiari, V.; Pistolis, G.; Lianos, P. *Chem. Mater.* **1999**, *11*, 3189. (b) Bekiari, V.; Pistolis, G.; Lianos, P. *J. Non-Cryst. Solids* **1998**, *226*, 200.
(14) Bekiari, V.; Ferrer, M.; Stathatos, E.; Lianos, P. *J. Sol−Gel Sci. Technol.* **1998**, *13*, 95.
(15) Yamaguchi, T.; Nomura, M.; Wakita, H.; Ohtaki, H. *J. Chem. Phys.* **1988**, *8*, 89.
(16) Guinier, A. *X-ray Diffraction*; Freeman and Company: San Francisco, 1993.
(17) Meakin, P. *The Fractal Approach to Heterogeneous Chemistry*; Avnir, D., Ed.; John Wiley and Sons: New York, 1989; p 131.
(18) Freltoft, T.; Kjems, J. K.; Sinha, S. K. *Phys. Rev. B* **1986**, *33*, 269.
(19) Teixeira, J. *J. Appl. Crystallogr.* **1988**, *21*, 781.

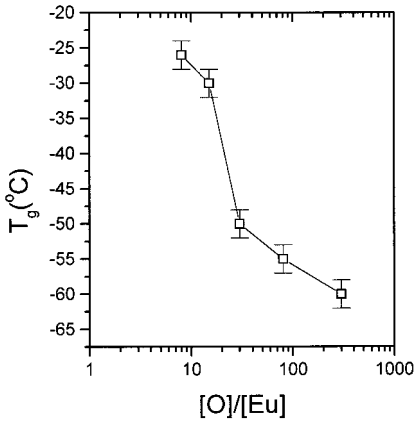

Figure 1. Glass transition temperatures of siloxane−PEG class I hybrids as a function of Eu^{3+} content.

Equation 4 represents the experimental scattering intensity produced by fractal aggregates up to q values equal to and even larger than $q_2 = 1/a$. Because of the approximation used for the form factor (eq 3), eq 4 does not reproduce the assymptotic Porod behavior expected at high q ($q \gg 1/a$).

More complex scattering functions are associated to structures with different types of spatial correlation at different scale levels. However, in the particular case of structures with well-defined spatial correlation within a small number of clearly different scales, the corresponding effects are concentrated in different q ranges and can eventually be identified.[20] In the following these basic concepts will be used to understand data obtained for high Eu^{3+} contents.

3. Results

3.1. Glass Transition. The temperature values obtained for glass transition (T_g) from TMA measurements are plotted in Figure 1. From low to moderate Eu^{3+} contents, that is, from $n = 300$ to $n = 30$, a small increase in T_g (−60 to −50 °C) is observed for increasing doping. For higher Eu^{3+} content ($n = 15$ and 8), T_g exhibits a strong increasing trend ($T_g = -25$ °C for $n = 8$).

These results suggest that the increasing addition of Eu^{3+} to the studied hybrids increases the rigidity of the structural network, this effect being particularly important for high Eu^{3+} concentrations ($n < 30$).

3.2. SAXS. Double logarithmic plots of the experimental scattering function $I(q)$ as a function of the scattering angle are displayed in Figure 2. For samples with $n = 300$ and 80 three different regions can be distinguished in the log−log plots of the scattering functions: (i) a nearly constant value at very small q, (ii) essentially linear behavior over the intermediate q range, and (iii) a crossover at high q. These features correspond to the scattering function of a set of isolated (non-inter-connected) fractal aggregates (eq 4).

The size parameter a of the primary particles, the correlation length ξ, and fractal dimension D of the aggregates were determined by fitting procedures of eq 4 to the experimental scattering curves. Satisfactory fits are obtained for the samples with lower Eu^{3+} content ($n = 300$ and $n = 80$). Deviations from the q dependence predicted by eq 4 are apparent for the $n = 15$ sample

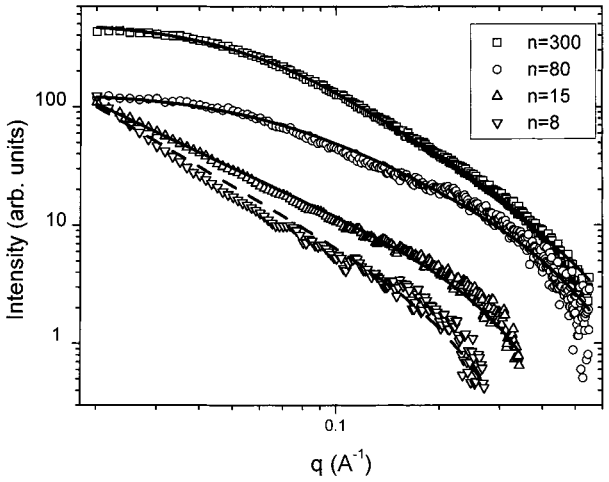

Figure 2. Experimental SAXS function $I(q)$ for siloxane−PEG class I hybrids class I xerogels with different Eu^{3+} contents (n). Continuous lines are the results of the fittings of eq 4 to the experimental curves corresponding to $n = 300$, 80, and 30. The dashed line illustrates the discrepancy between the theoretical prediction of eq 4 and the experimental results for high Eu^{3+} content ($n = 8$).

Table 1. Structural Parameters Derived from SAXS Results[a]

n ([O]/[Eu])	a (Å)	ξ (Å)	R_g (Å)	D
300	2.9	16	29	2.1
80	2.3	16	26	1.7
15	4.8	>100	>200	1.4

[a] a, radius of the primary particles; ξ, correlation length; R_g, radius of gyration; D, fractal dimension.

and a clear discrepancy occurs for the sample with $n = 8$. The values of a, ξ, R_g, and D determined by the best fitting of eq 4 for samples with $n = 300$, 80, and 15 are reported in Table 1.

The good agreement of the experimental SAXS intensity curves with the theoretical prediction of eq 4 indicates that the structure of the low Eu^{3+} content class I hybrids ($n = 300$ and 80) consists of small and isolated fractal aggregates ($R_g = 29-26$ Å) composed of primary particles having an average radius of 2.9−2.3 Å. The fractal dimensions obtained for these two hybrids are clearly different (2.1 for $n = 300$ and 1.7 for $n = 80$).

As stated before, the log−log plots of the experimental scattering functions corresponding to samples with $n = 15$ and 8 are clearly different from those presenting relatively low Eu^{3+} concentration. The linear behavior below $q < 0.05$ A^{-1} does not show any tendency to a constant value at very small q as predicted by eq 4 (Guinier range). This indicates that the scattering objects are very large so that the crossover q_1 lies at $q \ll q_{min}$.

In the case of the sample with $n = 15$ the utilization of eq 4 leads to a relatively poor fit. However, it can still be applied as a first approximation. The values so obtained for the radius of the primary particles ($a = 4.8$ Å) and the size of the aggregates ($R_g > 200$ Å) are larger than those obtained for samples with lower Eu^{3+} content.

The important deviation of experimental and theoretical SAXS curves for the hybrid with $n = 8$ (Figure 2) suggests that the model of isolated fractal aggregates does not apply to this sample with high Eu^{3+} content.

(20) Beaucage, G.; Ulibarri, T. A.; Black, E. P.; Schaeffer, D. W. *Hybrid Organic−Inorganic Composites*; American Chemical Society: Washington, D.C., 1995; Chapter 9.

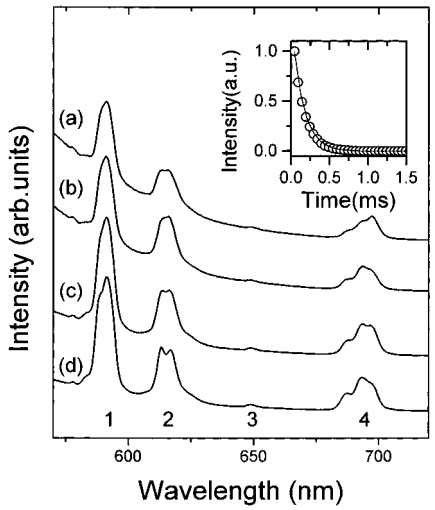

Figure 3. Room-temperature Eu^{3+} emission spectra obtained under 394-nm excitation for siloxane−PEG class I hybrids. (a) $n = 300$; (b) $n = 80$; (c) $n = 30$; (d) $n = 8$. Numbers under the curves denote J levels for the transitions $^5D_0 \rightarrow {}^7F_J$. Inset: typical Eu^{3+} $^5D_0$ emission decay curve observed for the sample $n = 30$. The line shows the fit obtained considering a single-exponential decay function ($\tau = 0.15$ ms).

A qualitative analysis of the experimental SAXS intensity suggests two clearly different q dependencies at low q ($q < 0.07$ Å^{-1}) and high q ($q > 0.07$ Å^{-1}). These different behaviors were assigned to a two-level spatial correlation model.[20] In this particular case this model consists of aggregates of primary particles building up large secondary aggregates. The experimental scattering function for $q > 0.07$ Å^{-1} contains information on the structure of the primary aggregates. The scattering function over the small q range, $q < 0.07$ Å^{-1}, provides structural information on the second level aggregates.

3.3. Luminescence and EXAFS. Figure 3 shows Eu^{3+} emission spectra obtained for the samples with different Eu^{3+} content. Eu^{3+} characteristic f−f transitions are observed superimposed on a broad emission band not studied in detail here. Emission arising mainly from the Eu^{3+} $^5D_0$ excited state to the $^7F_{0,1,2,3,4}$ manifolds is observed. Assignments were done by comparison with the literature and are also noted in Figure 3.

As a general observation, relatively broad and nonstructured bands are observed, suggesting the existence of a broad distribution of sites available for the Eu^{3+} ion in the composite medium. In addition, the magnetic dipolar $^5D_0 \rightarrow {}^7F_1$ transition displays the highest intensity in each spectrum. In contrast to what we have previously observed for class II hybrids,[8] no significant differences could be detected from spectra obtained for samples with different Eu^{3+} concentrations. Spectral lines display the same mean energy positions and relative intensities for the entire range of Eu^{3+} concentrations considered here. Some initial splitting seems to appear in the $^5D_0 \rightarrow {}^7F_2$ transition profile for the sample with $n = 8$ but the relative transition intensities are essentially the same. In class II hybrids significant variations were observed as a function of Eu^{3+} concentration.[8−10] Eu^{3+} $^5D_0$ decay times were also determined and the inset of Figure 3 shows a typical emission decay profile. Single exponential decay functions could be used to fit experimental data and decay times values so obtained are listed in Table 2. It is observed that decay times hardly change with Eu^{3+} concentration with values between 0.14 and 0.17 ms.

Table 2. Eu^{3+} $^5D_0$ Level Decay Time for Dried Gels Class I for Different Eu^{3+} Contents

n ([O]/[Eu])	decay time (±0.02 ms)	n ([O]/[Eu])	decay time (±0.02 ms)
8	0.15	80	0.17
15	0.14	300	0.14
30	0.14		

The first coordination sphere of Eu^{3+} was further characterized with X-ray absorption measurements. EXAFS data analysis was performed on a Macintosh microcomputer with the "A. Michalowicz's EXAFS pour le Mac" software.[21] The EXAFS signal $k\chi(k)$, where k is the wave vector for the photoelectron, was extracted from the raw absorption data using the Lengeler-Eisenberger method.[22] The $k\chi(k)$ spectra were Fourier transformed using k^2 ponderation and a Kaiser window ($\tau = 2.5$) leading to spectra scaled in distance (Å). The peaks in the Fourier transforms, $|F(r)|$, corresponding to each coordination shell were then filtered and back-transformed to k space. The resulting EXAFS-filtered signals have been treated as a sum of sinusoidal wave functions using plane wave and single scattering approximation,[23]

$$k\chi(k) = S_0^2 \sum_i \frac{N_i}{R_i^2} e^{-2\sigma_i^2} e^{-2R_i/\lambda(k)} f_{ij}(\pi,k) \sin[2kR_i + \Phi_{ij}(k)] \quad (6)$$

where N_i is the number of atoms in the coordination shell i at average interatomic distance R_i from the absorbing atom, σ_i is the Debye−Waller factor, which takes into account the static and thermal structural disorder, $\lambda(k)$ is the photoelectron mean free path, and S_0^2 is an amplitude reduction factor reflecting multielectron effects. $f_{ij}(\pi,k)$ and $\Phi_{ij}(k)$ are the amplitude and the phase functions for this coordination shell. In this case they were obtained experimentally from the standard Eu^{3+} perchlorate aqueous solution. The Fourier-filtered signal obtained were then simulated by a least-squares fitting procedure, leading to the determination of the structural parameters R, N, and $\Delta\sigma$ for the first coordination shell around the absorbing Eu^{3+} atom.

Experimental results are not shown here due to limiting space but just the Eu^{3+} first coordination shell could be characterized. No long range order could be observed. Mean values of 9.8 ± 0.5 for N, 2.41 ± 0.05 Å for d, and 0.12 ± 0.01 Å^2 for $\Delta\sigma^2$ were obtained with no appreciable differences in the range of samples studied.

4. Discussion

The results of the SAXS experiments indicate that the structure of the studied hybrids consists of aggregates embedded in a nearly homogeneous matrix. Since the polymer weight fraction was kept constant at the high 86 wt % value, we have assumed that the major phase

(21) Michalowicz, A. *EXAFS pour le Mac*; Societé Française de Chimie: Paris, 1991; p 102.
(22) Lengeler, B.; Eisenberger, P. *Phys. Rev. B* **1980**, *21*, 4507.
(23) Teo, B. K. *EXAFS: Basic Principles and Data Analysis*; Inorganic Chemistry Concepts Series; Springer: Berlin, 1986; Vol. 9.

is a polymeric matrix and that the minor one is composed of inorganic siloxane aggregates.

A number of studies of aggregation processes of colloidal particles in liquid solvents have demonstrated that, in many cases, fractal clusters are formed. On the other hand, computer simulations demonstrated that the fractal dimension of the cluster depends on the mechanism of aggregation.[17]

The experimental value of the fractal dimension $D = 2.1$ (Table 1) of siloxane aggregates in hybrids with low Eu^{3+} content ($n = 300$) suggests that the predominant mechanism of cluster formation during the gelation process is reaction-limited cluster−cluster aggregation (RLCCA).[24,25] This is the mechanism expected for our synthesis procedure in which the first step involves acid-catalyzed hydrolysis and the second one the addition of a base.[24] For medium Eu^{3+} content ($n = 80$) the fractal dimension is smaller ($D = 1.7$). This value is close to that determined by computer simulation for diffusion-limited cluster−cluster aggregation (DLCCA).

The difference in the aggregation mechanism for hybrids with Eu^{3+} content $n = 300$ and $n = 80$ suggests that Eu^{3+} ions enhance the sticking probability of primary siloxane particles during the aggregation−gelation process. This effect associated with the electrolyte has already been observed in other sol−gel-derived materials containing different salts.[26] In our case Eu^{3+} ions decrease the electrostatic repulsion between primary siloxane particles. Higher sticking probability for the primary particles with the increase in Eu^{3+} concentration would favor diffusion as the controlling mechanism for aggregation.

Clear structural differences are observed when samples with high Eu^{3+} content ($n = 15$ and 8) are compared to those with lower Eu^{3+} content ($n = 300$ and 80). In the case of the sample $n = 15$, the expected stronger effect of Eu^{3+} ions still decreasing the electrostatic repulsion between primary particles induces an aggregation process, leading to much larger aggregates ($R_g \gg 100$ Å). For the sample $n = 8$, this phenomenon leads to the formation of large secondary clusters themselves constituted by aggregates of primary siloxane particles. Figure 4 gives a general picture of the different situations for low and high Eu^{3+} content, showing in the last case the formation of larger aggregates.

This conclusion is consistent with the observed increase in the glass transition temperature for increasing Eu^{3+} content. As a matter of fact, the expected effect of the larger size of inorganic siloxane aggregates is to increase the overall structural strength of the composite.

Luminescence data can be compared with previous results obtained for similar materials in the literature[13,14] and also for related class II materials studied before.[8]

Bekiari et al.[13] studied Eu^{3+}-containing SiO_2-PEG_{200} hybrids prepared by acid-catalyzed hydrolysis of silicon alcoxides. The authors observed marked changes in emission spectra as a function of the relative polymer concentration. An enhancement of Eu^{3+} electric dipolar

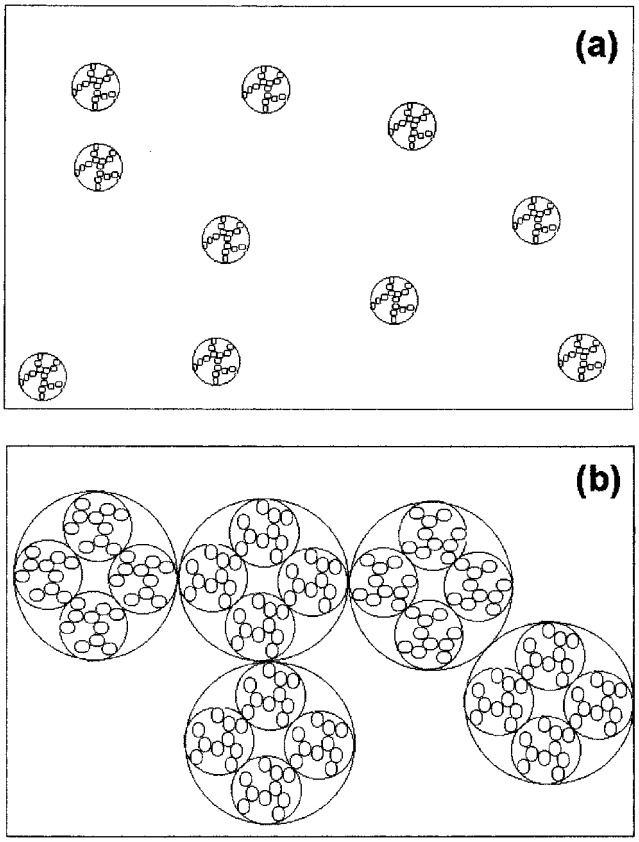

Figure 4. Schematic views of the proposed structure models of scattering siloxane particles in a polymer medium for (a) low and (b) high Eu^{3+} content.

transitions was first assigned to a cage-like environment provided by the polymer molecules which could protect Eu^{3+} from interactions with water molecules. The same authors[14] presented a systematic work with PEG_{200} and PEG_{400} and observed that emission enhancement was observed to occur in water for a polymer relative concentration above a critical polymer concentration of 80% in weight. The emission enhancement was observed to occur together with a $^5D_0$ lifetime increase. In siloxane−PEG mixtures the authors did not observe a critical polymer concentration. They reported a continuous increase in intensity and decay times values particularly for PEG_{200}. The effect was less pronounced for PEG_{400}.

It is interesting to note that different behavior is observed for our samples. Considering the spectra shown in Figure 3, the magnetic dipolar $^5D_0 \rightarrow {}^7F_1$ is the one presenting the highest intensity for all the samples. Additionally, the low values for the $^5D_0$ decay time in our samples reflect the interaction of Eu^{3+} ions with relatively high energy vibrational modes of the host (OH^-). In fact, despite the broad distribution of available sites for the Eu^{3+}, as suggested by the inhomogeneously broadened bands, decay curves could be fitted by single-exponential functions, showing that the decay rate is governed by nonradiative processes. These features indicate that for all samples the Eu^{3+} first coordination shell shows water-like behavior. The same behavior is known to occur for pure silica sols.[6]

The purely radiative contribution for the decay times can be evaluated using the magnetic dipolar $^5D_0 \rightarrow {}^7F_1$ transition as a reference, for which the Einstein's

(24) Brown, W. D.; Ball, C. D. *J. Phys. A* **1985**, *18*, L17−521.
(25) Jullien, R.; Botet, R. *Aggregation and Fractal Aggregates*; World Scientific: Singapore, 1987.
(26) Brinker, C. J.; Scherer, G. W. *Sol−Gel Science*; Academic Press: San Diego, 1990; p 203.

coefficient (A) of spontaneous emission is well-known ($\approx$50 s^{-1}) and does not depend on the crystal field. The other observed transitions arising from the $^5D_0$ level have electric dipolar character and therefore the total spontaneous emission coefficient (A_{TOTAL}) could be evaluated from band intensities. Transitions to the $^7F_{5,6}$ manifolds were not considered since they must present extremely weak intensity and could not be observed. The value of $\approx$180 s^{-1} was obtained for all samples and therefore the pure radiative lifetime, $\tau_{radiative}$, is around 5.5 ms. Experimental decay time values shown in Table 1 range from 0.14 to 0.17 ms. The differences between these values and those calculated can be assigned to significant contributions from nonradiative decay rates. In fact, emission quantum yields, expressed as the ratio of the experimental and radiative lifetimes, are very low ($\approx$3%). This picture together with the SAXS and EXAFS results can be considered by the interaction of Eu^{3+} with the siloxane particles surface which is a completely different situation from that found for class II hybrids.[8] In that case we could, from the experimental results, suggest the interaction of Eu^{3+} mainly with the ether-type oxygen atoms of the organic subphase.

The marked differences observed considering our results and those presented in the literature for related systems[13,14] are very instructive, showing that in fact spectroscopic properties should be largely dependent on the preparation procedures as well as on the nature of the precursors. Bekiari et al.[13,14] have been using acid-catalyzed hydrolysis throughout the whole preparation procedure; their Eu^{3+} precursor is a nitrate salt and PEG molecular weights were 200 and 400. Considering the hydrolysis process, it is well-known that completely different materials could be obtained by changing the catalysis mechanism.[26] Base catalysis used here in the gelation step could promote the interactions between Eu^{3+} and the negatively charged silanol groups present on siloxane particle surfaces. If that would be the case, this interaction could well account for the effect of the addition of Eu^{3+} proposed in the explanation of SAXS and TMA results. Moreover, it must be considered that the ability of nitrate ions, used by Bekiari et al.,[13,14] in coordinating to rare earth ions, is certainly higher than the one displayed by perchlorate ions used here in our work. In aqueous solution nitrate ions are known to be present in the Eu^{3+} first coordination shell which is not the case for perchlorate. The different nature of the Eu^{3+}-containing cationic species in water certainly has a significant effect on the spectroscopic properties of the final product. Finally, a significant effect was observed[13,14] for PEG_{200}, being less pronounced for PEG_{400}. Since we have been working with PEG_{600}, a dependence on the molecular weight could not be excluded, suggesting systematic work to be done.

5. Conclusion

As observed for undoped similar hybrids,[12] siloxane−PEG (MW = 600) class I nanocomposites with relatively low Eu^{3+} content (n = 300 and 80) are composed of a minor phase consisting of inorganic siloxane aggregates with a fractal structure and a major phase which is a homogeneous polymeric matrix. Fractal aggregates are built up by primary siloxane nanoparticles or groups. The addition of higher quantities of Eu^{3+} (n = 15) leads to a decrease in the interparticle repulsion interactions and the subsequent formation of larger aggregates. When the Eu^{3+} content (n = 8) is increased further, the reduction in electrostatic repulsion between siloxane aggregates due to the presence of Eu^{3+} ions at the particle surfaces induces an additional aggregation process, leading to the formation of very large secondary aggregates.

The different structural features deduced from SAXS results explain the observed increase in mechanical strength of the hybrids and consequent increase in the glass transition temperature for increasing Eu^{3+} content.

Luminescence spectra and structural features obtained from EXAFS suggest that under the experimental conditions used here Eu^{3+} ions experiment a water-like environment for the entire range of concentrations studied. The negatively charged surface of the siloxane nanoparticles could well account for those conditions and therefore establish relative insensitivity of Eu^{3+} ions to the organic subphase.

Acknowledgment. As noted by one of the referees of this paper, *Chemistry of Materials* has turned into an interesting vehicle for discussion of organic−inorganic hybrids. In this sense we would like to thank the referees for their important suggestions and even corrections for some misinterpretations in our results appearing in the original submitted version. The authors also acknowledge the collaboration of LNLS staff during the SAXS and EXAFS experiments and the financial support from Brazilian agencies FAPESP, PRONEX, and CNPq.

CM0012320